Low Velocity Impact Evaluation of Self-Healing Sandwich Structures

A.F.V. Pedroso[1,*], R.D.S.G. Campilho[1,2], R.J.B. Rocha[2] and M.A. Gomes[3]

[1]*Departamento de Engenharia Mecânica, Instituto Superior de Engenharia do Porto, Instituto Politécnico do Porto, R. Dr. António Bernardino de Almeida, 431, 4200-072 Porto, Portugal*

[2]*INEGI – Pólo FEUP, Rua Dr. Roberto Frias, 400, 4200-465 Porto, Portugal*

[3]*ISQ, Avenida Professor Dr. Cavaco Silva, 33 Taguspark, 2740-120 Porto Salvo, Portugal*

Abstract: One of the main problems within aeronautical industries is the collision, in low-flight, take-off and landing, between the fuselage of the aircraft and birds. This occurrence results in irreversible damage and consequent repairs of the composite material that composes the aircraft structure. The focus of this work is to find a solution that drastically reduces the lack of residual impact strength of composite materials, combining laminates of hybrid fibre fabrics from carbon with Dyneema® with a self-healing elastomeric adhesive Reverlink™ in a composite sandwich with a honeycomb core. Comparison is undertaken with a more traditional approach that considers the epoxy Araldite® 2015 adhesive instead. Low-velocity impact tests were made, and the experimental results enabled the comparison of both solutions. The test trials showed an improved impact behaviour of the Reverlink™ solution and regeneration after the first impact. Thus, the proposed solution can be considered instead of traditional sandwich joining with epoxy adhesives.

Keywords: Self-Healing material, Low-velocity impact, Reverlink™, Hybrid composite, Sandwich.

1. INTRODUCTION

There has been a huge focus on the study of new solutions for polymeric materials, due to their lower mechanical strength and susceptibility to damage [1]. Self-healing polymeric materials can be separated into two mechanisms [2]: (1) autonomous: the materials, which can be doped, start the regeneration process based on the energy transmitted by the fracture performed, and (2) non-autonomous: the materials are only able to initiate the regeneration process after the fracture using external stimuli. Focusing on autonomous materials, there are two types of self-regeneration. The first type is intrinsic, including thermally reversible covalent bond (TRCB) polymers, ionomers, supramolecular chemical-based materials (such as hydrogen bonding), thermosetting resin with unreacted epoxide, and polymers with dynamic covalent bond exchange (DCBE) [3, 4]. For any of these variants, the activation energy will always come from the cracking, and no external activation energy is required. The second type is extrinsic, divided into structural and conventional thermosetting polymer matrices, and shape memory polymer (SMP) matrices with the close-then-heal (CTH) approach. In this case, there is a need for doping with an external regeneration agent, such as microcapsules [5], whose regenerator is a base of urea-formaldehyde, hollow fibres and biomimetic microvascular networks [4, 6, 7].

Fatigue and impact in composite materials poses an added challenge, in the design of solutions, given their heterogeneous nature [8]. According to Ismail, *et al*. [9], the ranges of impact velocities (v) are discretized as follows: (1) low-velocity impact (LVI) if $v \leq 10$ m/s, medium velocity impact (MVI) if $10 < v \leq 50$ m/s, and high-velocity impact (HVI) if $50 < v \leq 1000$ m/s. For the application of composite materials in impact situations, the highest possible fracture toughness is recommended, as this will ensure greater and better absorption of energy from the impact. Specifically, in the case of carbon fibres, it is generally found that the higher the tensile strength (σ_u), the greater the energy required to propagate the crack (G_c) [10, 11]. According to the literature, some composite systems are particularly suited for impact applications, such as Dyneema®, carbon fibre (CF) and glass fibre (GF) with Hexcel HexFlow® RTM6 epoxy resin [12], Dyneema®/aluminium with epoxy resin [13], heterocyclic aramid fibre reinforced plastics (HAFRP) with 315 K epoxy resin [14], carbon fibre/Nomex® honeycomb with epoxy resin [15], and GF/Reverlink™ HR-NR (HN-50-NC) with Araldite LY 8615 epoxy resin [16]. Heimbs, *et al*. [12] experimented, through three types of tests (Charpy, drop-weight and ballistic), the behaviour of CF, GF and Dyneema® laminates

*Address correspondence to this author at the Departamento de Engenharia Mecânica, Instituto Superior de Engenharia do Porto, Instituto Politécnico do Porto, R. Dr. António Bernardino de Almeida, 431, 4200-072 Porto, Portugal; Tel: +351 916154627; E-mail: andre.pedroso@outlook.pt

subjected to impact. The authors concluded that comparing the normalized penetration energy, the Dyneema® laminate with 24-plies and $[0°/90°]_{12}$ layup had a better performance in the ballistic test. GF, on the other hand, had a slightly better performance than Dyneema® in the remaining tests. CF had the worst performance. Sordo and Michaud [16] presented a study of GF laminates with two different matrices: Reverlink™ HR-NR (HN-50-NC) and epoxy resin (Araldite LY 8615), to compare them in dynamic mechanical analysis (DMA). The GF/Reverlink™ laminate was also tested in a three-point bending test and LVI. In flexural tests, self-healing had an efficiency after 24 h time (η_{24h})=65% of mechanical strength, and 72% of flexural stiffness was recovered. In the LVI test (with 20 J), it was possible to observe the complete self-regeneration of the elastomeric matrix after 28 days.

The focus of this work is to find a solution that drastically reduces the lack of residual impact strength of composite materials, combining laminates of hybrid fibre fabrics from carbon with Dyneema® with a self-healing elastomeric adhesive Reverlink™ in a composite sandwich with a honeycomb core. Comparison is undertaken with a more traditional approach that considers the epoxy Araldite® 2015 adhesive instead. Low-velocity impact tests were made, and the experimental results enabled the comparison of both solutions.

2. MATERIALS AND METHODS

2.1. Framework and Methodology

This research is part of the MOSHO project, which is intended to develop and integrate advanced solutions for repairing aeronautical structures in composite materials. The fundamental objective of this work is to study, evaluate and characterize the dynamic behaviour of self-healing sandwich structures subject to low-velocity impact loads, and to verify the strength and stiffness recovery. Subsequently, a second impact test campaign will be carried out in order to characterize the energy absorption behaviour after self-healing. Initially, thermo-mechanical tests were performed to characterize the applied materials, *i.e.*, Dynamic Mechanical Analysis and Differential Scanning Calorimeter tests. After the specimens' manufacture, drop weigh impact tests were performed.

2.2. Materials

The selected material for the face sheets was the Dyneema® Carbon DDCFX005 (Torayca FT300-40B and Dyneema® SK99) fabric, whose main characteristics are given in Table **1** and Table **2**.

The material was impregnated at SHD composites (UK) with MTC510 epoxy resin. Additionally, the prepreg mechanical properties were evaluated at INEGI facilities. Table **3** summarizes the obtained properties.

Table 1: Construction Characteristics of Dyneema® Carbon DDCFX005

Construction	Warp	Weft
Yarn Material	Dyneema® SK99/Torayca FT300-40B	
Twill ratio Dyneema®/CF	1:2	
Yarn number Dyneema®/CF	880/2000 dtex	
Dyneema® Content in Weight	18 wt%	
Weave	2/2 Twill	

Table 2: Dyneema® Carbon DDCFX005 Characteristics

Property		Typical Value
Setting	Warp [thread/cm]	6.0
	Weft [thread/cm]	6.0
Fabric Areal Weight – FAW [g/m^2]		195
Moisture Content [%]		Max. 0.5

Table 3: Dyneema® Carbon DDCFX005 Mechanical Properties

Standard	Property	Measured Values
ASTM D3039/D3039M – 14	E_{11}, E_{22} (T)	47.61 GPa
	σ_{1t}, σ_{2t}	523.26 MPa
ASTM D3518/D3518M – 13	G_{12}	3.55 GPa
	τ_{12}	83.33 MPa
ASTM D6641/D6641M – 16^{e1}	E_{11}, E_{22} (C)	32.64 GPa
	σ_{1c}, σ_{2c}	161.70 MPa
ASTM D7291/D7291M – 15	E_{33}	2.00 GPa
	σ_{3c}	11.64 MPa
ASTM D5379/D5379M – 12	G_{23}	2.07 GPa
	τ_{13}, τ_{23}	84.88 MPa
ASTM D5528 – 13	DCB, G_{Ic}	0.91 N/mm (kJ/m^2)
ASTM D7905/D7905M – 14	ENF, G_{IIc}	1.79 N/mm (kJ/m^2)
ASTM D3846 – 08 (2015)	DEN (T)	198.19 N/mm (kJ/m^2)
	DEN (C)	5.00 N/mm (kJ/m^2)
ISO 14130:1997(E)	ILSS, τ^0_{SH}	31.73 MPa
	ν_{12c}, ν_{13c}	0.04 [-]
	ν_{12t}, ν_{13t}	0.04 [-]

Caption: C – compression; DCB – double cantilever beam; DEN – double-edge notched; E_{11} – longitudinal modulus of elasticity; E_{22} – transverse modulus of elasticity; E_{33} – out-of-plane transverse modulus of elasticity; ENF – end-notched flexure; G_{12} – transversal shear modulus, in plane 12; G_{23} – transversal shear modulus, in plane 23; G_{Ic} – Fracture toughness for mode I fracture; G_{IIc} – Fracture toughness for mode II fracture; ILSS – interlaminar shear strength; T – traction; ν_{12} – Poisson coefficient, in plane 12; ν_{13} – Poisson coefficient, in plane 13; σ_{1t} – Longitudinal tensile stress; σ_{2t} – Transverse tensile stress; σ_{1c} – Longitudinal compression stress; σ_{2c} – Transverse tensile stress; σ_{3c} – Transverse compression stress, direction 3; τ^0_{SH} – interlaminar shear stress; τ_{12} – Shear stress, in plane 12; τ_{13} – Shear stress, in plane 13; τ_{23} – Shear stress, in plane 23.

The Nomex® honeycomb (reference A1-3-64:A1), supplied by I.MA.TEC (Italy) was selected for the core. The dimensions and general characterizations of the honeycomb are listed in Table **4**.

Table 4: Characteristics of the used Nomex® Honeycomb

Density=64 kg/m^3	The thickness of the wall cell (t)=0.12 mm
Cell size (w)=3 mm	Overall thickness=10 mm

The Nomex® honeycomb elastic properties were calculated taking into account the hexagonal cell's geometry and the analytical model by Malek and Gibson [17], and are presented in Table **5**.

Table 5: Elastic Properties of the used Nomex® Honeycomb

E_1=0.45315 MPa	G_{12}=0.11331 MPa	ν_{12}=0.99557
E_2=0.45382 MPa	G_{13}=38.618 MPa	ν_{13}=0.00051
E_3=257.98 MPa	G_{23}=63.106 MPa	ν_{23}=0.00051

Arkema® (FR) supplied the Reverlink™ HR-NR, elastomeric material to be used as adhesive, bonding the skins and the honeycomb core. The recommended cure cycle is 130°C for 12 hours. The resulting product presents a supramolecular hybrid network composed of 50% of hydrogen bonds and 50% of covalent bonds. Few tests were carried out including self-healing capabilities and adhesion. A comparison was made between the Reverlink™ and the adhesive Araldite® 2015 (ductile epoxy), which was formerly tested regarding the mechanical and fracture properties [18].

2.3. Specimen Details and Impact Testing

Sandwich panels with 150×100 mm^2 were manufactured (Figure **1**). The sandwich consists of two skin sheets, each has five layers, with the formerly mentioned layup of [(45,-45)/(45,-45)/(90,0)/(45,-45)/(45,-45)]. The overall thickness of the skin (five plies) is 1.25 mm and the Nomex® honeycomb core thickness is 10 mm. Reverlink™ was used to adhere the honeycomb with the two skins.

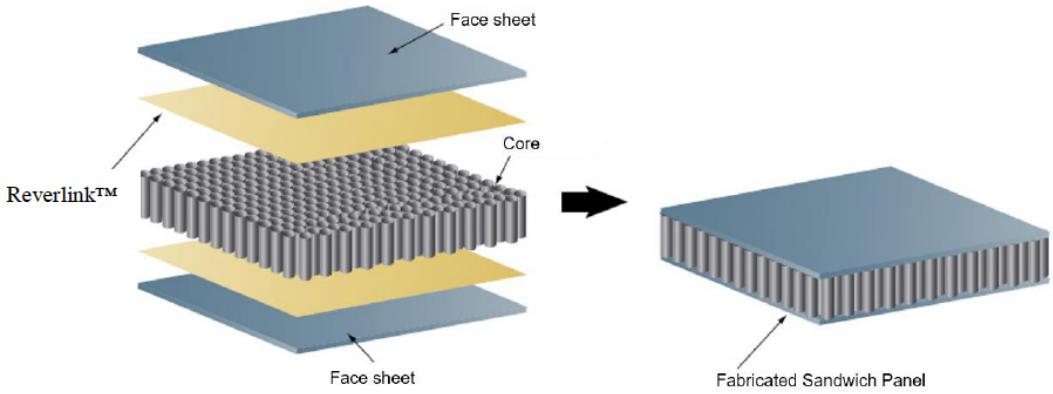

Figure 1: Sample of a sandwich panel with Reverlink™.

The sandwich skins were manufactured by the following steps:

- Cutting the laminae for skin fabrication;
- Manually stacking the laminae that form the skins with the defined layup;
- Curing the skins in an oven with the manufacturer's temperature and pressure indications;
- Cutting the skin laminates and core in a diamond disc saw to the individual specimen dimensions;
- Reverlink™ spreading in the laminate, after reaching a temperature of 100ºC, manually using a spatula, or Araldite® 2015 spreading in the laminate at room temperature after manual mixture of the two parts of adhesive;
- Assembly of the skins/core;
- Curing in a oven after isolating the specimens with Teflon® film to avoid Reverlink™ spreading;
- Trimming the edges to the final specimen dimensions.

The apparatus used for the drop-weight impact test is illustrated in Figure **2**. The procedures inherent to the test are found in the ASTM D7136/D7136M – 15 standard [19], which can be consulted for further details. This standard requires that at least five valid specimens be tested. To evaluate the Reverlink™ self-regeneration, two tests of 20 J are recommended for

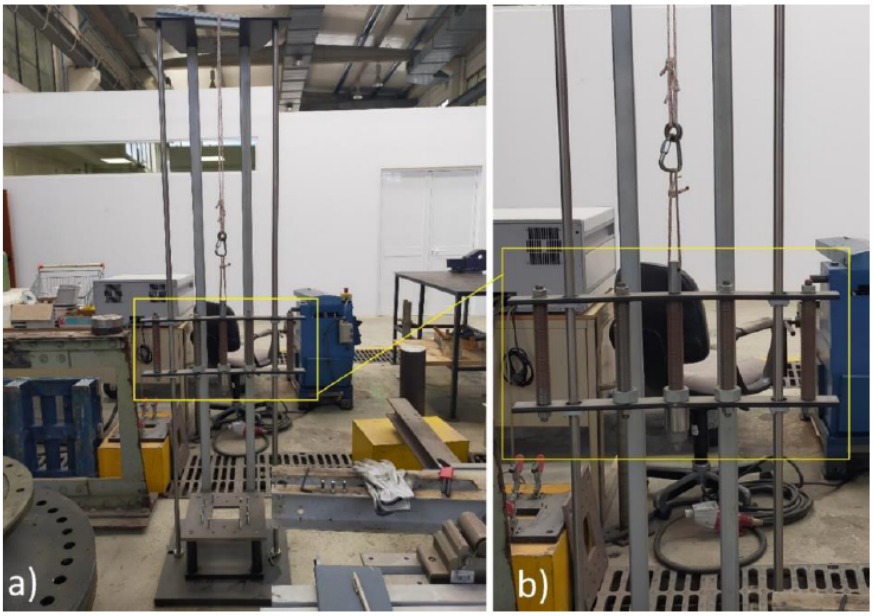

Figure 2: Drop weight impact test: (**a**) setup and (**b**) impactor tip and mass detail.

each sandwich structure and the following procedures were implemented:

1. The first LVI test applied to the sandwich structures caused a loss of mechanical strength, as well as stiffness. From here damage area (A_{damage}) and maximum depth ($\downarrow_{damage}$) are measured;

2. A 24h conditioning at a temperature (T) of 90°C was carried out to accelerate the self-healing process of Reverlink™, as described by Sordo and Michaud [16];

3. The second LVI test was performed 24h after the self-healing initiation. A_{damage} and $\downarrow_{damage}$ were measured once again.

3. RESULTS

3.1. Visual Analysis of the Failed Specimens

Figure **3** shows a visual comparison between specimen 1 with Reverlink™ and with the only specimen with Araldite® 2015, both tested to a 20 J LVI. In Figure **3**(**a**), it is visible that the Nomex® core is exposed, having resulted from the penetration, which caused the laminate fracture. In Figure **3**(**b**), core exposure is not observable. In this case, only perceptible fracture and Dyneema® matrix debonding were found, resulting from compression effects and CF crushing.

Figure **4** provides the visual comparison of the resulting damage between the 1st LVI (a) and the 2nd LVI (b), having Reverlink™ specimen 1 as an example.

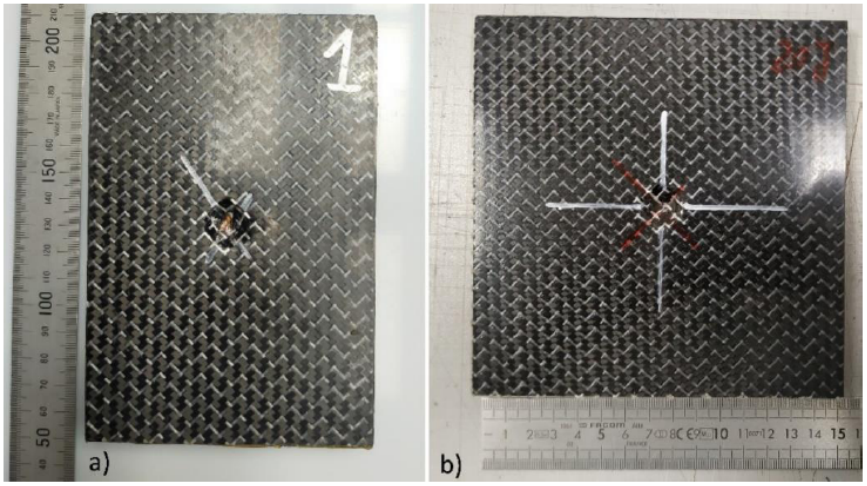

Figure 3: Sandwich drop-weight specimen with **a**) Reverlink™ specimen 1; **b**) Araldite® 2015.

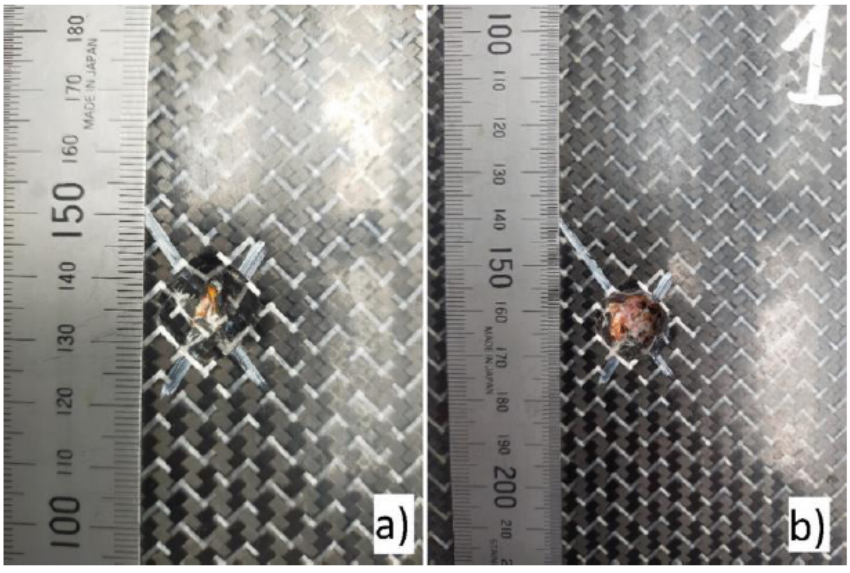

Figure 4: Reverlink™ specimen 1, front face after (**a**) 1st LVI, (**b**) conditioning and 2nd LVI.

Table 6: Values of the Various LVI Parameters, and A_{damage} and $\mathcal{I}_{damage}$, in the First Drop-Weight Test, for the Five Sandwich Structures with Reverlink™

Specimen	Impact Conditions					Damage after 1st Impact		
	$Ø_{esf}$ (mm)	m (kg)	h (m)	v_i (m/s)	E_i (J)	Penetration	A_{damage} (mm²)	$\mathcal{I}_{damage}$ (mm)
1	12.50	11.46	0.178	1.87	20.00	Yes	243.30	7.72
2							238.70	8.19
3							223.20	4.11
4							261.00	8.06
5							244.40	6.29

Legend: A_{damage} – damaged area; h – free fall height; m – impact assembly mass; $\mathcal{I}$ – maximum depth; $Ø_{esf}$ – hemispherical impactor diameter.

The core exposure to the exterior is compared between Figure **4**(**a**) and (**b**), which is more significant after the 2nd LVI, and it is patent the complete laminate fracture due to a 2nd Dyneema® fibre crushing and to matrix cracks, visible in the damaged perimeter (P_{damage}).

3.2. Impact Test Data Analysis

Table **6** presents the values obtained of A_{damage} and $\mathcal{I}_{damage}$ to the sandwich structures with Reverlink™. E_i is the applied impact energy.

Having Reverlink™ as a cohesion element between the laminates and honeycomb core, a median damage area ($\bar{X}_{Adamage}$) of 242.12 mm² was measured in the sandwich impact surface, with a sample standard deviation of damage area ($s_{Adamage}$) of 13.53 mm² and a coefficient of variation of damage area ($\%s_{Adamage}$) of 5.59%. For $\mathcal{I}_{damage}$, a median value ($\bar{X}_{\mathcal{I}\,damage}$) of 6.87 mm was obtained, with a sample standard deviation ($s_{\mathcal{I}}$) of 1.72 mm and a coefficient of variation ($\%s_{\mathcal{I}}$) of 25.02%. The high value of $\%s_{\mathcal{I}}$ is mainly due to specimen 3. Table **7** presents A_{damage} and $\mathcal{I}_{damage}$ for the sandwich structures with Araldite® 2015, tested to three different E_i values. Comparing the data of specimen 02-20J (although there is no statistically equal representation for E_i=20 J) with the Reverlink™ data, lower values of A_{damage} were obtained for the Reverlink™ case, as it is shown in Table **8**.

The values of ΔA_{damage} exalt the absorption and damping energy capacity of Reverlink™ since the 20 J LVI could not translate into an equal value of A_{damage} nor destruction of the sandwich structure with Araldite® 2015. After 24h conditioning to the sandwich structures

Table 7: Values of the Various LVI Parameters, and A_{damage} and $\mathcal{I}_{damage}$, in the Single Drop-Weight Test, for the Four Sandwich Structures with Araldite® 2015

Specimen	Impact Conditions					Damage after only Impact		
	$Ø_{esf}$ (mm)	m (kg)	h (m)	v_i (m/s)	E_i (J)	(1)	A_{damage} (mm²)	$\mathcal{I}_{damage}$ (mm)
02-10J-1	12.50	11.46	0.089	1.32	10.00	No	78.54	NE
02-10J-2			0.089	1.32	10.00	No	78.54	NE
02-20J			0.178	1.87	20.00	Yes	314.16	NE
02-30J			0.267	2.29	30.00	Yes	314.16	NE

Legend: (1) penetration; NE – not evaluated.

Table 8: A_{damage} Values, from the first Drop-Weight Test, for the Five Sandwich Structures with Reverlink™, and Respective Differences, $\Delta_{Adamage}$, with the Specimen with Araldite® 2015

	Araldite® 2015	Reverlink™				
Specimen	02-20J	1	2	3	4	5
A_{damage} (mm²)	314.16	243.30	238.70	223.20	261.00	244.40
ΔA_{damage} (mm²)	[-]	-70.86	-75.46	-90.96	-53.16	-69.76

Legend: ΔA_{damage} – damage area differential.

Table 9: Values of the Various LVI Parameters, and A_{damage} and $\mathcal{I}_{damage}$, in the Second Drop-Weight Test, for the Five Sandwich Structures with Reverlink™

Specimen	Impact Conditions					Damage after 2nd Impact		
	$Ø_{esf}$ (mm)	m (kg)	h (m)	v_i (m/s)	E_i (J)	Penetration	A_{damage} (mm²)	$\mathcal{I}_{damage}$ (mm)
1	12.50	11.46	0.178	1.87	20.00	Yes	243.30	9.88
2							238.70	10.06
3							223.20	11.18
4							261.00	10.30
5							244.40	9.86

with Reverlink™, at T=90°C, the 2nd LVI test is fulfilled. Table **9** highlights the impact conditions, identical to the 1st LVI, and both A_{damage} and $\mathcal{I}_{damage}$. Comparison of A_{damage} to those of Table **6** shows identical values. In the $\mathcal{I}_{damage}$ domain, the presented values are expectedly higher, compared with the 1st LVI, obtaining a $\bar{X}_{\mathcal{I}\,damage}$ of 10.26 mm. Moreover, $s_{\mathcal{I}}$ value of 0.55 mm and a $\%s_{\mathcal{I}}$ value of 5.32% were attained, which demonstrates that the consequences of a 2nd LVI resulted in higher repeatability.

Analysing the difference of maximum depth values ($\Delta\mathcal{I}_{damage}$) depicted in Table **10**, it is possible to conclude that there was a quantity of Reverlink™ that flowed towards the places where the impact took place, aiming at filling possible cracks with the elastomer to dampen and restore some local mechanical strength and stiffness. This phenomenon is reflected in the $\Delta\mathcal{I}_{damage}$ values, which are lower than the $\mathcal{I}_{damage}$ values obtained in the 1st LVI, excepting specimen 3.

Analysing the $\Delta\mathcal{I}_{damage}$ values from Table **10** it is possible to affirm that there was self-healing activity from Reverlink™ due to the conditioning, otherwise, the values of $\mathcal{I}_{damage}$ from the 2nd LVI would be double from the 1st LVI values. In this case, it is known that Reverlink™ efficiently self-heals 65% within 24 hours (η_{24h}), hence $\Delta\mathcal{I}_{damage}$ values obtained don't represent 30 % of the 1st LVI $\mathcal{I}_{damage}$ values obtained in specimens 1,2 and 4 and 50 % in specimen 5.

3.3. Discussion and Comparative Evaluation

In the present study of the 150×100 mm² Reverlink™ sandwich structures, subjected to a drop-weight impact, it was found that A_{damage} values were smaller than for the homologous specimen with Araldite® 2015, since the Reverlink™ elastomer has a higher capacity to dissipate energy due to its high ε_u value. Nevertheless, it was found that, in all sandwich structures with Reverlink™, when penetrated, the Nomex® core was always exposed and visible to the naked eye (except in specimen 3), which was not visible in the specimen 02-20J with Araldite® 2015. This difference is intrinsically related to the resilience modulus (U_r) of the Araldite® 2015. While the Reverlink™ has a higher capacity to dissipate energy in the plastic regime or better toughness, the Araldite® 2015 has better resilience due to the significantly higher Young's modulus. In the self-healing domain, the same is verifiable through $\mathcal{I}_{damage}$ values obtained for the 1st and 2nd LVI events of the sandwich structures with Reverlink™. The different behaviour between the Reverlink™ and Araldite® 2015 sandwich structures

Table 10: Values of $\mathcal{I}_{damage}$, from the First and Second Drop-Weight Tests, for the Five Sandwich Structures with Reverlink™, and Respective Differences

Specimen	1st Impact	2nd Impact	
	$\mathcal{I}_{damage}$ (mm)	$\mathcal{I}_{damage}$ (mm)	$\Delta\mathcal{I}_{damage}$ (mm)
1	7.72	9.88	2.16
2	8.19	10.06	1.87
3	4.11	11.18	7.07
4	8.06	10.30	2.24
5	6.29	9.86	3.57

can also be explained in light of the work of Sordo, *et al*. [20], which comparatively tested Reverlink™ with another Araldite® adhesive (Araldite® LY 8615 + Aradur® 8615) with similar characteristics to the Araldite® 2015. It was argued by the authors that, due to the elastomeric nature of Reverlink™, this material has a higher capacity to cushion the impact, compared to the Araldite® adhesive solution, which is defined as a ductile structural epoxy adhesive. It can therefore be stated that, due to its stiffer behaviour, the Araldite® 2015 does not have the necessary capacity to cushion impacts, nor the ability to dissipate energy, through plastic deformation, that Reverlink™ has, translating into higher damage levels and greater dissipation of energy in the form of material destruction. Another expedient way to compare the two materials could be through the storage modulus (*E*'), loss modulus (*E*'') and damping coefficient (tan *δ*), although there is no reference in the literature of DMA tests to Araldite® 2015.

4. CONCLUSIONS

The present work addressed the typical lack of residual strength of composite materials to impact loadings, by combining carbon/Dyneema® composites in a sandwich structure with Nomex® core and Reverlink™ as joining material. The trials essentially showed that the specimens joined with Reverlink™ had a significant A_{damage} reduction, when compared to specimens joined with Araldite® 2015 (up to approximately 90% for a single specimen), due to the higher energy absorption and damping of this material. The 2nd impact of the Reverlink™ joined sandwich structures revealed no changes in the 1st impact value of A_{damage}. Moreover, by analysing $\Delta \mathcal{I}_{damage}$ between both impacts, a significant reduction was found compared to the initial $\mathcal{I}_{damage}$, showing that regeneration took place. However, in the Reverlink™ structures, the Nomex® core was always exposed, due to the smaller resilience modulus of Reverlink™, compared to the Araldite® 2015. In general, it is considered that the Reverlink™ can improve the impact characteristics of sandwich structures over an epoxy adhesive, and that 2nd impact regeneration takes place. Thus, this innovative material can be an effective replacement of epoxy adhesives for composite sandwich structures under impact loads, by effectively reducing the lack of residual strength of impacted sandwich structures.

REFERENCES

[1] W. Kejian, J. Zhicheng, Z. Zhongfeng, P. Gaolin, J. Honggang, and S. Zhengtao, "Improved viscoelastic damping properties of carbon black reinforced EPDM composites by blending with ENR," Journal of Composites and Biodegradable Polymers, vol. 8, pp. 28-33, 2020. https://doi.org/10.12974/2311-8717.2020.08.4

[2] M. Mobaraki, M. Ghaffari, and M. Mozafari, "3 - Self-healing polymers for composite structural applications," in Self-Healing Composite Materials, A. Khan, M. Jawaid, S. N. Raveendran, and A. M. Ahmed Asiri Eds. Sawston, Reino Unido: Woodhead Publishing, 2020, pp. 33-51. https://doi.org/10.1016/B978-0-12-817354-1.00003-X

[3] S. J. Garcia, "Effect of polymer architecture on the intrinsic self-healing character of polymers," European Polymer Journal, vol. 53, pp. 118-125, 2014/04/01/ 2014. https://doi.org/10.1016/j.eurpolymj.2014.01.026

[4] G. Li and H. Meng, "1 - Overview of crack self-healing," in Recent Advances in Smart Self-healing Polymers and Composites, G. Li and H. Meng Eds. Sawston, Reino Unido: Woodhead Publishing, 2015, pp. 1-19. https://doi.org/10.1016/B978-1-78242-280-8.00001-7

[5] D. Y. Zhu, M. Z. Rong, and M. Q. Zhang, "4 - Microcapsule-based self-healing materials," in Recent Advances in Smart Self-healing Polymers and Composites, G. Li and H. Meng Eds. Sawston, Reino Unido: Woodhead Publishing, 2015, pp. 101-127. https://doi.org/10.1016/B978-1-78242-280-8.00004-2

[6] E. Archer and A. McIlhagger, "15 - Repair of damaged aerospace composite structures," in Polymer Composites in the Aerospace Industry (Second Edition), P. Irving and C. Soutis Eds. Sawston, Reino Unido: Woodhead Publishing, 2020, pp. 441-459. https://doi.org/10.1016/B978-0-08-102679-3.00015-0

[7] M. Mobaraki, M. Ghaffari, and M. Mozafari, "2 - Basics of self-healing composite materials," in Self-Healing Composite Materials, A. Khan, M. Jawaid, S. N. Raveendran, and A. M. Ahmed Asiri Eds. Sawston, Reino Unido: Woodhead Publishing, 2020, pp. 15-31. https://doi.org/10.1016/B978-0-12-817354-1.00002-8

[8] H. S. Kim, "Theory and Practical Procedure for Predicting SN Curves at Various Stress Ratios#," J. Compos. Biodegrad. Polym, vol. 7, pp. 57-72, 2019. https://doi.org/10.12974/2311-8717.2019.07.8

[9] M. F. Ismail, M. T. H. Sultan, A. Hamdan, A. U. M. Shah, and M. Jawaid, "Low velocity impact behaviour and post-impact characteristics of kenaf/glass hybrid composites with various weight ratios," Journal of Materials Research and Technology, vol. 8, no. 3, pp. 2662-2673, 2019/05/01/ 2019. https://doi.org/10.1016/j.jmrt.2019.04.005

[10] J. Lamon, "3 - Reinforcement of ceramic matrix composites by ceramic continuous fibers," in Composite Reinforcements for Optimum Performance (Second Edition), P. Boisse Ed. Sawston, Reino Unido: Woodhead Publishing, 2021, pp. 55-93. https://doi.org/10.1016/B978-0-12-819005-0.00003-4

[11] M. Shao *et al*., "On mode I/II interlaminar fracture toughness of double-sided-loop 2D woven laminated composites," Compos. Struct., p. 115311, 2022/01/29/ 2022. https://doi.org/10.1016/j.compstruct.2022.115311

[12] S. Heimbs, T. Wagner, JT. Viana Lozoya, B. Hoenisch, and F. Franke, "Comparison of impact behaviour of glass, carbon and Dyneema composites," Proc. Inst. Mech. Eng., Part C, vol. 233, no. 3, pp. 951-966, 2019. https://doi.org/10.1177/0954406218764509

[13] M. Zakeri, H. Mansoori, M. Sadeghian, and M. Guagliano, "Impact response of fiber metal laminates based on aluminum and UHMWPE composite: Numerical simulation," Thin-Walled Structures, vol. 172, p. 108796, 2022/03/01/ 2022. https://doi.org/10.1016/j.tws.2021.108796

[14] C. Wang *et al*., "Dynamic behaviour of Bio-inspired heterocyclic aramid Fibre-reinforced laminates subjected to Low-velocity Drop-weight impact," Composites Part A:

Applied Science and Manufacturing, vol. 153, p. 106733, 2022/02/01/ 2022. https://doi.org/10.1016/j.compositesa.2021.106733

[15] X. Zhang, F. Xu, Y. Zang, and W. Feng, "Experimental and numerical investigation on damage behavior of honeycomb sandwich panel subjected to low-velocity impact," Compos. Struct., vol. 236, p. 111882, 2020/03/15/ 2020. https://doi.org/10.1016/j.compstruct.2020.111882

[16] F. Sordo and V. Michaud, "Processing and damage recovery of intrinsic self-healing glass fiber reinforced composites," Smart Materials and Structures, vol. 25, no. 8, p. 084012, 2016/07/14 2016. https://doi.org/10.1088/0964-1726/25/8/084012

[17] S. Malek and L. Gibson, "Effective elastic properties of periodic hexagonal honeycombs," Mechanics of Materials, vol. 91, pp. 226-240, 2015. https://doi.org/10.1016/j.mechmat.2015.07.008

[18] C. L. Ferreira, R. Campilho, and R. D. F. Moreira, "Experimental and numerical analysis of dual-adhesive stepped-lap aluminum joints," Proceedings of the Institution of Mechanical Engineers, Part E: Journal of Process Mechanical Engineering, vol. 234, no. 5, pp. 454-464, 2020/10/01 2020. https://doi.org/10.1177/0954408920905747

[19] ASTM D 7136/D 7136M - 15. Standard Test Method for Measuring the Damage Resistance of a Fiber Reinforced Polymer Matrix Composite to a Drop-Weight Impact Event, ASTM, Pennsylvania, USA, 2015.

[20] F. Sordo, L. Berret, B. Caglar, and V. Michaud, "Impact Recovery of Self-Healing Composites Based on a Supramolecular Polymer Matrix," 2017.

Received on 23-11-2022 Accepted on 20-12-2022 Published on 30-12-2022

DOI: https://doi.org/10.12974/2311-8717.2022.10.04